Chapter 4

Study of Photoluminescence of Polyaniline grafted Graphene Oxide (GO-PANI) nanocomposite: Effect of pH

4.1. Introduction

The presence of different oxygen containing functional groups such as epoxide, carboxylic acids, hydroxyl group in graphene Oxide (GO), makes tremendous attention to the researcher to synthesis different types of GO-based composite materials by interacting with different organic and inorganic materials. In our experimental work, we have interested on conductive polymer like polyaniline (PANI) to synthesis GO-based composite materials because of its facile synthesis and wide environment friendly industrial applications due to desirable electrical, electrochemical and optical properties [1-24]. PANI is nothing but a class of conjugated polymer with extended π-conjugated structure. But PANI is unique in the sense that its electrical properties can be controlled by protonation of the imine nitrogen atoms and by changing the oxidation state of the main chain using the dopant acids [5]. The hydrophilic sate of PANI (emeraldine state, ES) is obtained in presence of doped acid which contains highly delocalized charge carriers and it is electrically conducting. Polyaniline can exist in three isolable oxidation states as "salts" or "bases", leucoemeraldine (LEB-white/clear or LES-colorless), emeraldine (EB-green or ES-blue), and pernigraniline (PB-blue or PS-violet), among which emeraldine salt (ES) is partially oxidized form of polyaniline .The various forms of polyaniline are shown in [Fig.1].Thus, PANI may be a promising candidate for developing graphene based nanocomposite material. Various nanostructures of PANI with excellent thermal, electrical and mechanical properties offer potential applications in different fields [6-7]. On the other hand, unlike graphene, GO is an electrically insulating material. The oxidized portion of GO actually disrupt the sp^2 bonding network of graphene and generate a large number of defect sites on its surface. Preparation of reduced graphene oxide by thermal reduction may decrease these defects and in consequence, the electrical properties of graphene can be restored [8]. Apart from thermal processes, there are also chemical processes which can help the restoration process [8-10]. One of them is the formation of Graphene oxide-polyaniline

(GO-PANI) nanocomposite [9-10]. This new type of functional nanocomposite (GO-PANI) based on graphene oxide has extensively been studied to produce materials with desired electrochemical properties [9-13]. The polar oxygen coating groups on the surface of GO make it dispersible in aqueous medium and may interact with the polar portion of polymer resulting in intercalated or exfoliated GO-polymer nanocomposites [12]. The exfoliation of GO results a larger surface area which enable strong interactions with PANI than that of tubular carbon nanotubes resulting in superior thermal and electrical properties [13]. Again, the conductivity of GO-PANI nanocomposites depends on the addition of dopant acids [11,13] and also on the weight ratio of GO to aniline [9]. Several groups reported that the in situ protonation of the aniline in GO-PANI nanocomposites have been made by the addition of external acids [9,11, 13]. Rana et al. reported a synthetic method for emeraldine salt formation of PANI by using the carboxylic acid of GO as a dopant acid rather than using any additional acids [9]. In the GO-PANI nanocomposite, GO is actually an excellent template for aniline nucleation and polymerization to form nanotube through possible interactions like π–π stacking, electrostatic interactions, hydrogen bonding and donor–acceptor interactions. In the nanocomposite, GO is getting reduced to form reduced graphene oxide resulting enhancement in electrical conductivity [9]. Maser and co-workers carried out in situ polymerization and subsequent reduction for the preparation of reduced GO-PANI by using 1:1 GO to aniline ratio where the simultaneous reduction of GO sheets covered by a thin layer of PANI leads to formation of a solid state charge transfer complex between reduced GO and PANI [14]. According to them, the formation of charge transfer complex is responsible for the enhanced conductivity of the material and the material is highly stable as well as dispersible in water with enhanced conductivities [14]. Kumar et al reported an alternative route for the preparation of conducting PANI grafted reduced GO composite having very high electrical conductivity [15]. Considering the advantage of the simple synthetic methodology, we synthesized PANI grafted

GO (GO-PANI) with a weight ratio of GO: aniline as 10:1 and studied the pH dependent tunable photoluminescence.

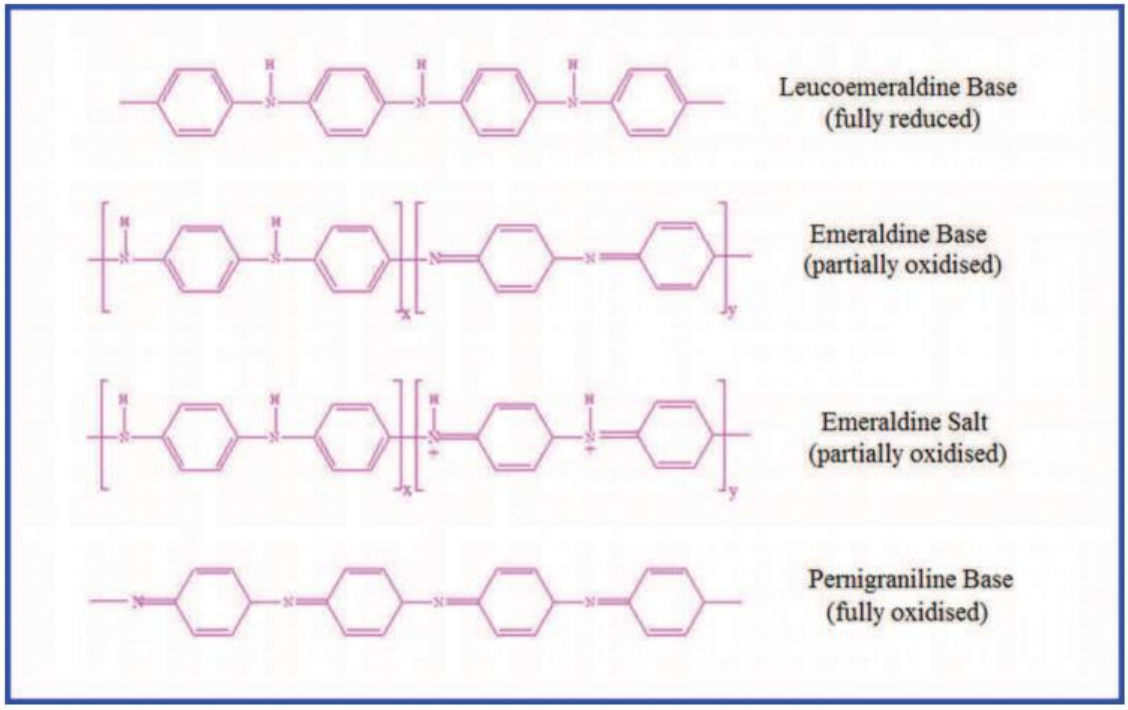

Fig. 1 Different oxidation form of PANI

4.2. Experimental Section

Powder XRD spectra (1.54 Å, Cu-Kα radiation) were recorded using a diffractometer at room temperature. The FTIR spectra were recorded using FTIR-680 plus (Jasco) at room temperature. Absorption spectra were recorded on a Hitachi U-4010 spectrophotometer at room temperature. The steady state emission and fluorescence excitation spectra were measured using a Hitachi Model F-7000 spectrofluorimeter equipped with a 150-W xenon lamp. The lifetime of the GO-PANI dispersion was measured by using TCSPC from PTI, USA, with the help of sub-nanocond pulsed LED source (280 nm having a pulse width of 600 ps). The pulsed LED source of 280 nm was operated at 10 MHz repetition rate driven by a PDL 800-B driver,

Pico Quant, Germany. LED profile was measured at the excitation of 280 nm with a band pass of 3 nm using Ludox as the scatterer. Decay measurements using "magic angle" detection with an emission polarizer set at 54.7° were carried out. The decay parameters were measured using nonlinear iterative fitting procedure based on the Marquard algorithm [16].The concentrations of GO and GO-PANI dispersions for the spectroscopic (UV-Visible absorption and emission) were 0.01 mg/ml.

4.2.1. Material and Method

The material required and the method of synthesis of GO-PANI has been discussed details in chapter 3 in section 3.2.

4.3. Result and Discussion

4.3.1. Characterisation

The GO-PANI has been characterised by different spectroscopic technique has been discussed details in chapter 3 with figure. Now, we interpret the characterisation result of our synthesized nanomaterial.

In the Raman spectra of GO-PANI [Fig. 2(a), chapter 3] it was observed that the nature of the spectrum is slightly different from that of GO [17]. The ratio of D band and G band is about 1 for GO [17] indicating the higher defect due to smaller size of graphene sheets in the nanocomposite [7, 18]. The intensity ratio of the two peaks at 1390 cm^{-1} and 1570 cm^{-1} in GO-PANI, is lower than GO and its value about 0.9. This suggests that the low defect in the GO sheets of GO-PANI in comparison to GO only and this may be interpreted as the chemical restoration by the growth of PANI chains on the GO layers to produce the GO-PANI nanocomposite. The observation of the peak at 1095 cm^{-1} may be explained as a down shifted of C-H bending of the quinoid benzenoid ring indicating the growing of the PANI chains on the surface of GO [19]. However, other peaks from PANI were not observed because of overlapping with GO peaks and small mole ratio PANI with respect to GO. The FT-IR

spectrum of GO-PANI also was found to be significantly different from that of GO [Fig. 2(b), chapter 3]. The peak about at ~ 1045 cm^{-1} which is due to C-O stretching indicates the similarity of the nanocomposite with GO. Again, the complete disappearance of the peak at 1724 cm^{-1} which is characteristic feature of C=O stretching of carboxylic acid in GO-PANI, suggesting two types of possibilities. First one is the possibility of complete reduction of GO during the synthesis of GO-PANI nanocomposite [9-10]. But, the important fact to be noted that we did not add any additional reducing agent [14] or excess aniline like Rana et al [9] during the preparation of the nanocomposite. Second possibility of the absence of the band nearly at 1700 cm^{-1} may be due to the overlapping of this weak band [Fig. 1(b), chapter 3] shifted towards the lower frequency by deprotonation of carboxylic acid group, with the quinoid band, which was strong enough. However, the presence of both quinoid and benzenoid band (with comparatively high intensity) may be attributed to the fact that the oxidation sate of PANI in the GO-PANI nanocomposite is emeraldine. The characteristic N-Q-N-Q band around 1150 cm^{-1} and the lower intensity of the quinoid band with respect to benzenoid band clearly supports that the partially reduced PANI is grafted on the surface of GO sheets [15]. Again, the shoulder at 1240 cm^{-1} may be attributed to the C-N stretching near the polaronic structure of emeraldine salt which has a small but finite contribution in the PANI [20]. Thus, the spectral results of both Raman and FTIR are suggesting that the GO-PANI nanocomposite is consists of few characteristic bands of both GO and PANI along with a property of polaronic structure in the aqueous dispersion which was acidic in nature (pH = 4.6).The most interesting observation in the XRD spectrum of GO-PANI [Fig. 2(c) in chapter 3] is the complete disappearance of GO peak and presence of PANI peak in the nanocomposite, indicating no aggregation of GO in the GO-PANI nanocomposite [11,15]. However, XRD spectrum of both GO and GO-PANI exhibits sufficient disorderness in spite of some periodicities. A weak peak which is appeared at $2\theta = 7^0$ may be interpreted as broadening of interlayer spacing, compared

to GO, possibly due to some little intercalation of PANI between the basal planes of GO by the reaction induced complete exfoliation of GO layers [15,21]. Thus, the XRD patterns finally supported the fact that PANI was grafted on the surface of GO in GO-PANI nanocomposite. To analysis the presence of different functional groups in GO-PANI nano-composite we may compare FT-IR and XPS data. In the FT-IR spectrum of GO-PANI, the observed peaks at 1299, 1497, 1570 cm^{-1} can be assigned to the characteristic peak related to C–N stretching near 2° amine, C=C stretching of benzenoid and quinoid rings, respectively, for PANI like characteristic peaks.The characteristic N-Q-N-Q band around 1150 cm^{-1} and the lower intensity of the quinoid band with respect to benzenoid band clearly supports that the partially reduced PANI is grafted on the surface of GO sheets. A band at 1240 cm^{-1} may be attributed to the C-N stretching near the polaronic structure of emeraldine salt. XPS of C1s and N1s [Fig. 2(a) and 2(b)] elucidate different electronic states and so different functional groups present in the GO-PANI nano-composite. Fig. 2(a) shows the C1s spectra of GO-PANI, which can be deconvoluted into four peak components: carbon sp^2 at 284.5 eV, indicating C-C group, carbon sp^3 at 285.4 eV, indicating C=C group, alkoxy C-O group at 286.8 eV and O-C=O group at 291.5 eV. Peaks for C-N group and C=O group are not clearly observed may be due to overlapping with the peak at 286.8 eV. The N1s XPS [Fig. 2(b)] can be deconvoluted into three peaks which include benzenoid amine with 399.5 eV binding energy and quinoid amine with 400.6 eV and 405.6 eV binding energies. The peak centered at 400.6 eV is due to nitrogen cationic radical present in the polyemeraldine salt. Both TEM and SEM images of GO-PANI also indicates the formation of a new type of nanocomposite [Fig. 2(d) and Fig. 2(e) of chapter 3] compared to GO [17]. This change may be due to adsorption and intercalation of PANI on the GO surface and between GO layers. Thus the characterization by Raman, FTIR, XRD, SEM and TEM is confirming the formation of a new kind of GO-PANI nanocomposite which is neither similar to GO nor resemble to PANI.

Fig. 2

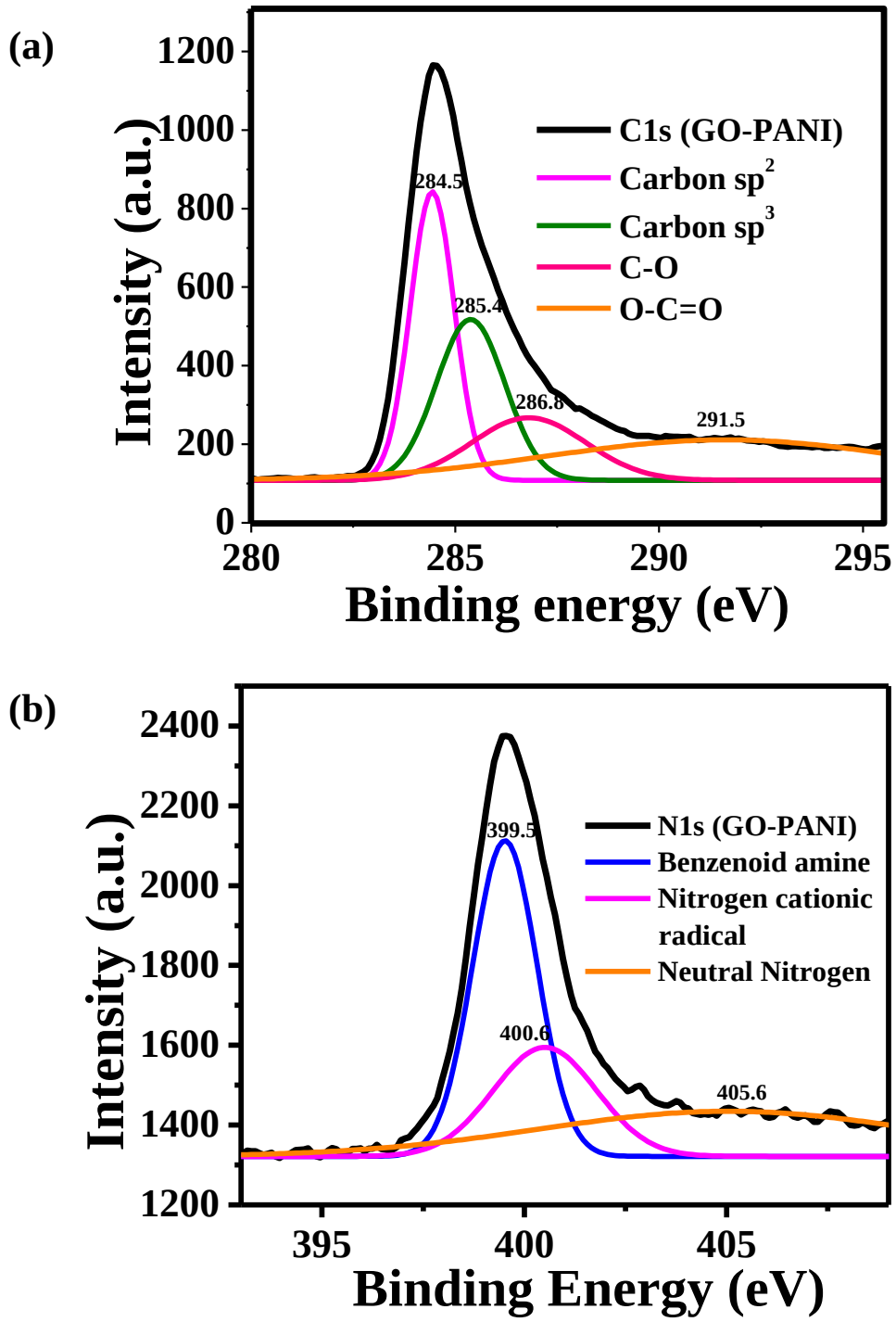

XPS of in GO-PANI: (a) Deconvoluted C1s spectrum (b) Deconvoluted N1s spectrum

4.3.2. Steady State Absorption Spectra

In the UV-Vis absorption spectra of the aqueous dispersion of GO-PANI, distinct features at different pH is observed as PANI is a mixed oxidation state polymer, ranging from the most reduced leucoemeraldine form to the half oxidized emeraldine and fully oxidized pernigraniline [22] [Fig. 3(a)]. Thus, the switching among these oxidation states and optical properties of PANI are interlinked and directly influences its UV-Vis absorption properties [23]. Emeraldine is green in colour. In this context, we want to mention that the colour of our GO-PANI nanocomposite is green indicating the oxidation state of the PANI chain as a form of emeraldine. In acidic pH, the absorption band at 436 nm indicates the characteristic polaron to π^* transition of the PANI moiety [9,14,24] which suggest that the PANI exist in polyemeraldine salt form. Another peak at 276 nm is observed due to n-π^* transition of GO moiety [17] present in GO-PANI nanocomposite. At pH = 4.6, a peak around 227 nm at pH = 4.6 resembles to π-π^* transition of GO moiety (Fig. 3b). Apart from this, the pH of the medium affects the optical properties of the emeraldine form of PANI by protonation and deprotonation of the basic sites (-NH-) which results the switching of PANI between different oxidation states [25]. This clearly suggests that the oxidation states of PANI are pH dependent. Hence, the transitions between oxidation states of PANI are accompanied by visible optical color change [25]. The absorption spectrum of GO-PANI (Fig. 3a) at the alkaline pH (10.7) shows a π-π^* band at the wavelength of 347 nm as a characteristic of the emeraldine base form of PANI [24, 26] and a strong absorption band at ~ 600 nm may be attributed to a local charge transfer between a quinoid ring and the adjacent imine-phenyl-amine units (intramolecular charge transfer exciton) [24, 27]. Here, it should be noted that the emeraldine base form of PANI has a structure consisting of almost equal proportion of amine and imine sites. In the acidic medium (pH = 1.8 and 4.6), imine sites are protonated to the bipolaron (dication salt) form [28] and then the bipolaron undergoes a further rearrangement to form the delocalized polaron [24]. In

consequence, the absorption band of GO-PANI around 600 nm is completely disappeared in acidic medium and the formation of polaron state at this low pH is confirmed by the appearance of an absorption band at 436 nm [Fig. 3(a)] which may be due to the transition from polaron state to π* [14,24]. This pH dependent absorption process is illustrated in [Fig. 4].

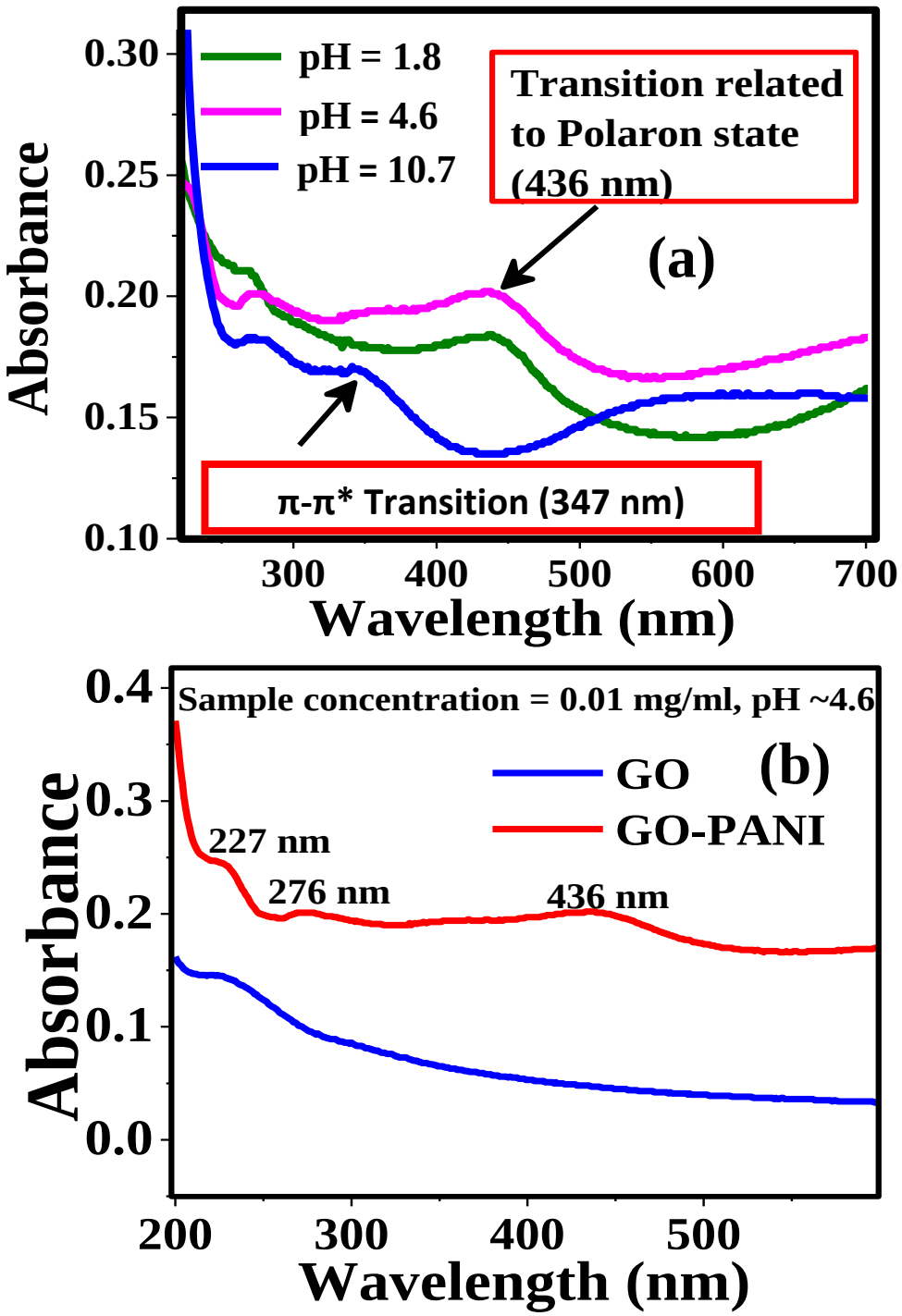

(a) Absorption Spectra of GO-PANI at different pH (220 nm – 700 nm)
(b) Absorption spectrum of diluted stock dispersion of GO and GO-PANI having concentration 0.01 mg/ml (pH ~ 4.6, 220 nm – 600 nm)

Fig. 4

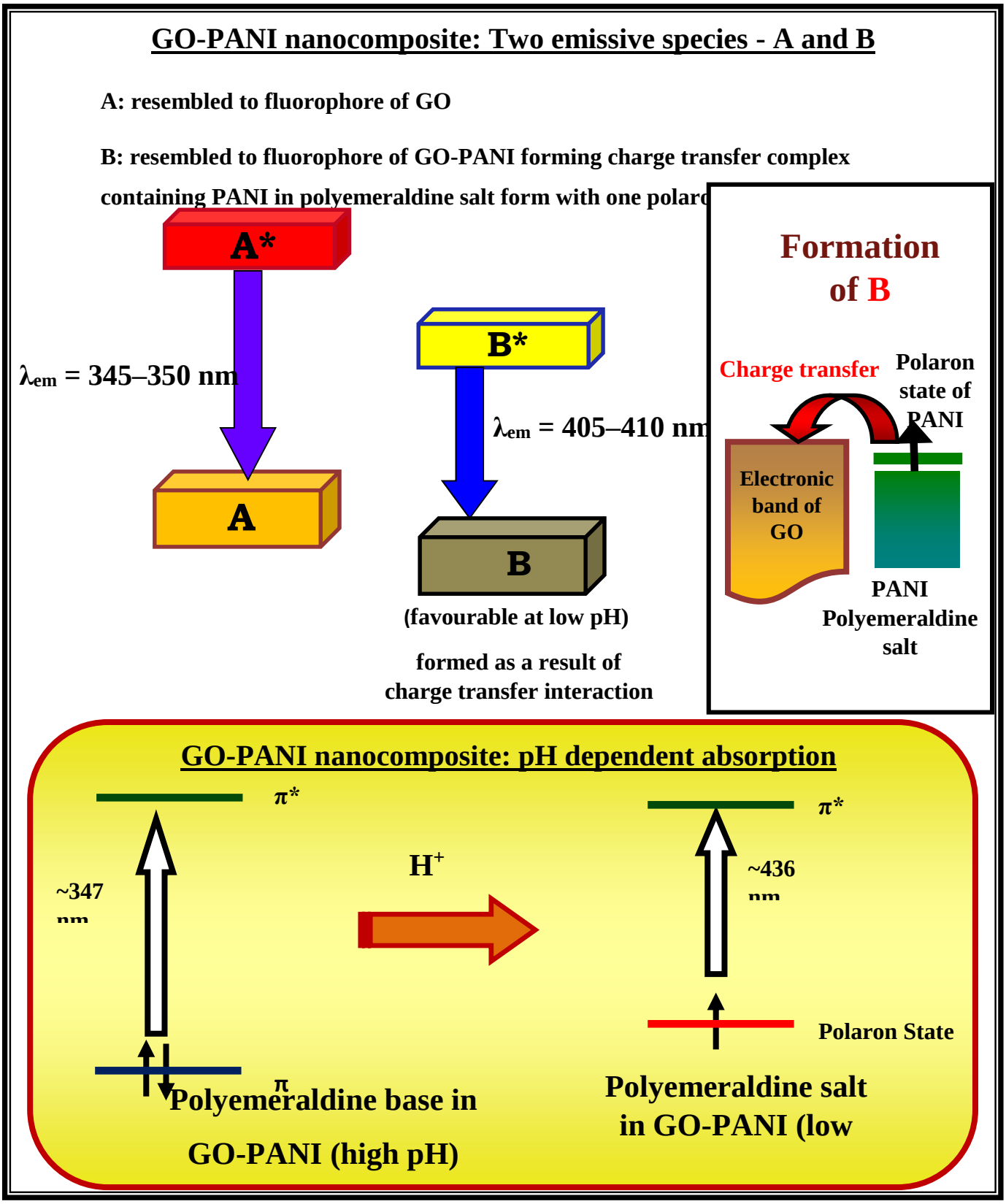

Schematic diagram for the absorption-emission processes in GO-PANI: Formation of Charge Transfer Complex

4.3.3. Steady State Emission Spectra

The luminescence behaviour of GO-PANI dispersion shows interesting features dependent upon the excitation wavelength and pH, due to the intrinsic inhomogenity and electronic band structure of the nanocomposite based on GO grafted by PANI. In this experiment, we excited the GO-PANI dispersion at π-π* band (230 nm) and at n-π* band (280 nm) of GO moiety by varying the pH of the medium from acidic region (pH = 1.8) to alkaline region (pH = 10.7). Excitation at 230 nm (pH = 1.8) results a broad and weak emission centered at about 410 nm [Fig. 5]. But, when the pH of the medium was above 3, the emission maxima of GO-PANI was obtained at 345 nm [Fig. 5] which was same as the fluorescence spectrum of the dispersion of GO [17]. In case of the excitation at 280 nm, a dual emission (two peaks at 345 nm and 405 nm) was observed at pH = 4.6 [Fig. 6(a)]. This indicates the possibility of the presence of two types of emissive species. But at low pH (less than 3) and at high pH (greater or equal to 7), single emission band was appeared instead of dual emission band. The center of the emission bands at low (less than 3) and high (greater or equal to 7) pH was obtained at 410 nm and 345 nm, respectively. This observation is suggesting the change in relative contribution of two types of fluorophoric moieties present in the aqueous medium at two different pH regions [Fig. 6(a)].

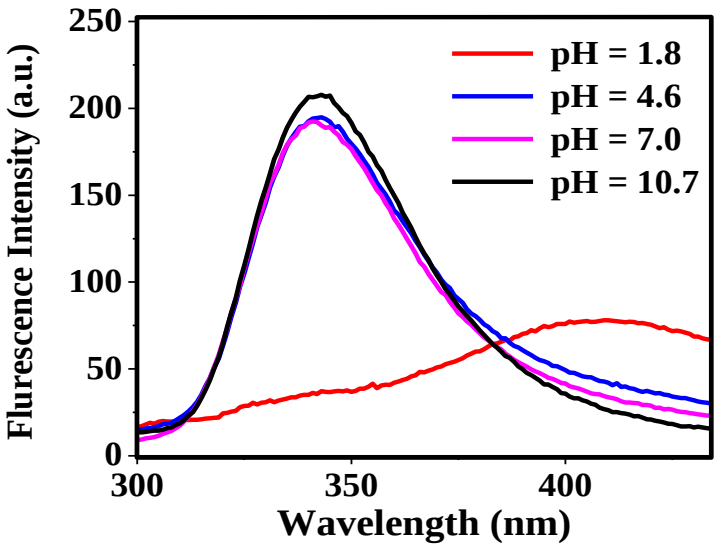

Fig. 5 Emission Spectra of aqueous dispersion of GO-PANI (λ_{ex} = 230 nm)

The 3D Contour plot of the emission of GO-PANI at different pH (λ_{ex} = 280 nm) [Fig. 6(b)] shows that the relative contribution of the emissive species changes with change in the pH of the medium and this leads to change in fluorescence intensities as well as a shift in emission maxima from visible region (410 nm) to UV region (345 nm) with the increase in pH.

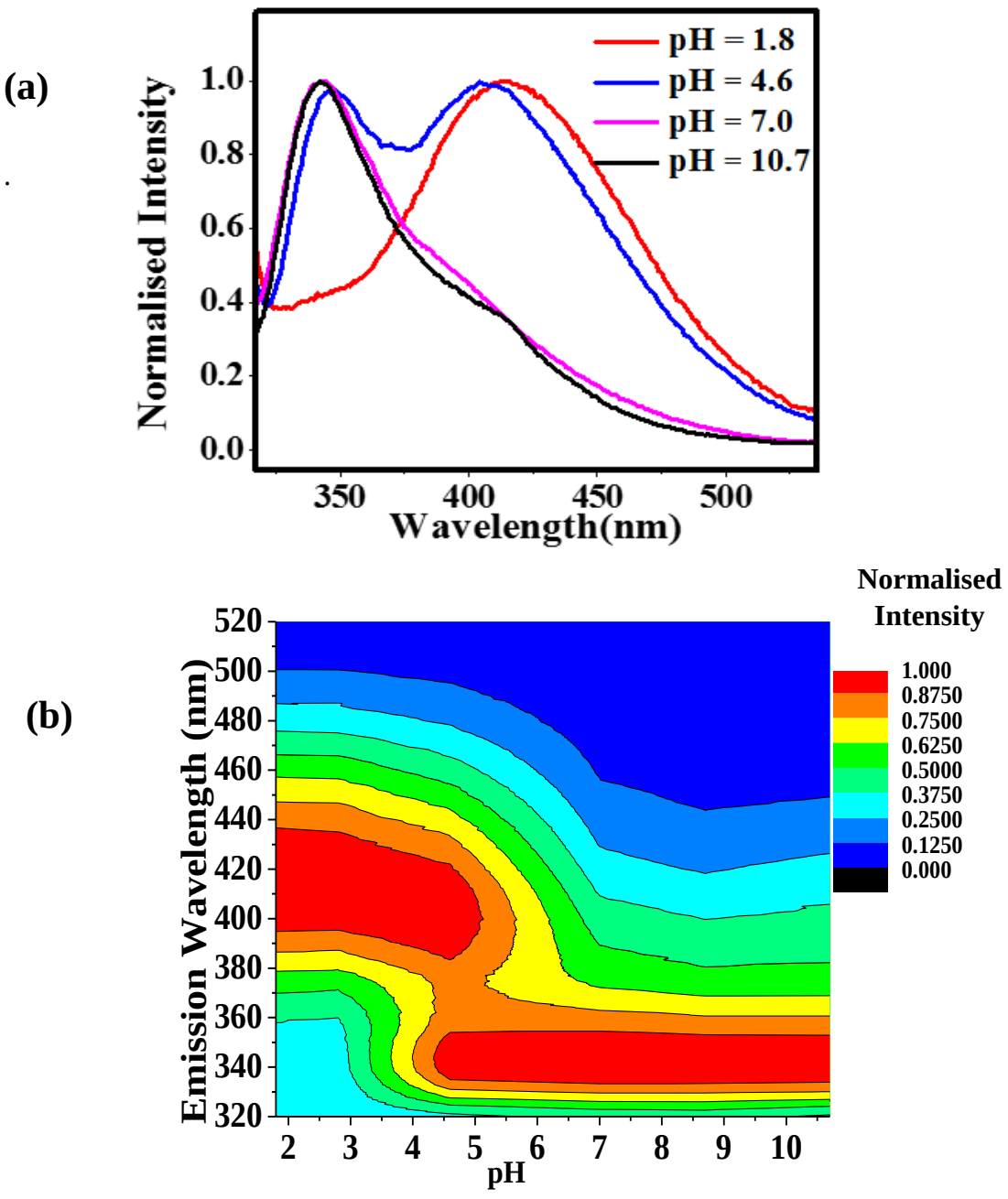

Fig. 6 (a) Emission Spectra of aqueous dispersion of GO-PANI (λ_{ex} = 280 nm)

(b) 3D Contour Plot: Emission of GO-PANI at different pH (λ_{ex} = 280 nm)

[Fig. 7(a)] exhibits the emission spectrum of GO-PANI at pH = 4.6 with two deconvoluted Gaussian like bands centered at 345 nm and 410 nm (λ_{ex} = 280 nm). Plot of emission intensities of two deconvoluted bands against pH of the aqueous dispersion of GO-PANI [Fig. 7(b)] suggests that the species exhibiting fluorescence peak at 345 nm, has very small contribution at low pH. On the other hand, gradual decrease in fluorescence intensity of the emission band centered at 410 nm, with the increase in pH [Fig. 7(b)] may be due to the decrease in the relative contribution of the moiety emitting at visible region. In this context, it should be mentioned that PANI shows no significant emission in the concerned pH range (1.8 – 10.7) if the aqueous dispersion of PANI is excited at 230 nm or 280 nm.

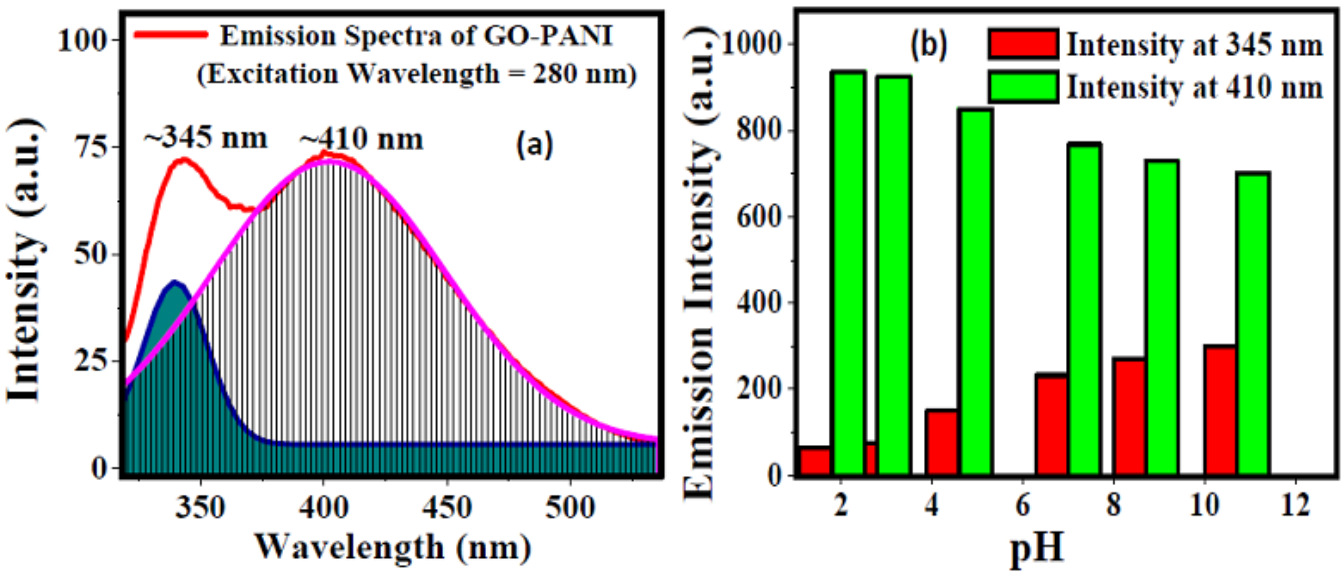

Fig. 7 (a) Emission spectrum of GO-PANI at pH = 4.6 with two deconvoluted Gaussian Like bands centered at 345 nm and 410 nm (λ_{ex} = 280 nm)

(b) Plot of emission intensities of two deconvoluted bands against pH of the aqueous dispersion of GO-PANI.

Thus, we observed that both the absorption and emission spectra are affected by the change in pH of the medium. To explain the pH dependencies in fluorescence spectra, people usually think about the excited state proton transfer or protonation-deprotonation of fluorophores. According to Zhang and coworkers, the dual fluorescence of GO in visible region was dependent upon excitation wavelength and pH of the medium [29]. They observed the very small change in absorption of GO by pH variation but significant change in emission properties of GO as a result of the excited state protonation and deprotonation and the pH sensitive functional groups at the GO surface. But, the change in absorption spectra as well as excitation spectra with the change in pH, only be explained by the formation of different ground state species. Like other carbon materials, such as C_{60} or SWNT, graphene as well as GO is an excellent electron acceptor [14, 30]. Thus, considering the electron donating ability of aniline [7], one may consider the electron donor-acceptor or charge transfer interaction within the GO-PANI nanocomposite. Maser and co-workers proposed that the electronic properties of reduced GO and an intermediate oxidation state of PANI results a charge transfer interaction between PANI and reduced GO [14]. According to them, the vast surface area of reduced GO sheets favors the contact between reduced GO and PANI and there by the charge transfer processes at the contact interface of reduced GO and PANI [14]. They added a reducing agent, hydrazine, for the in situ reduction of GO. But, in our work, no external reducing agent was used. Hence, we are proposing a different mechanism. It is well known that there is equilibrium between the emeraldine base and emeraldine salt in the aqueous medium containing H^+ ion and this equilibrium is influenced by the pH of the medium. In alkaline medium, PANI exists as emeraldine base form and this is confirmed by the absorption spectrum. With the decrease in the pH, formation of emeraldine salt form with polaron state becomes favorable [24]. In consequence, unstable single electron in the polaron state of PANI transfers charge to the extended conjugated backbone of GO sheets [Fig. 4] which are capable to store negative

charges like graphene layers in graphite intercalation compound [31]. Hence, as a result of charge transfer interaction along with π-π interaction [9], a ground state complex [B in Fig. 4] may be formed in acidic pH. The ground state and the excited state of the fluorophore of the partially charge separated species, B, becomes stable in aqueous polar medium and this leads a red shifted emission band at 410 nm. But, in alkaline medium, no such polaron states are formed and so usual emission resembled to GO is observed. Thus, in acidic pH, the luminescence property of GO-PANI nanocomposite is changed due to various interactions like electrostatic charge transfer interaction, π-π stacking which actually modulate the π-electronic band structure of GO by the formation of a species, denoted as B [Fig. 4].

4.3.4. Excitation Spectra

The fluorescence excitation (FLE) spectra monitored at 345 nm and 410 nm at acidic (1.8) and alkaline pH (10.7) exhibit interesting features [Fig. 8(a) and 8(b)]. In alkaline pH (pH = 10.7), FLE spectra monitored at 345 nm, shows two peaks at 230 nm and 280 nm. The peak at 280 nm is due to n-π* transition of GO moiety [Fig. 8(b)]. But, in acidic pH (pH = 1.8), the peak at 250 nm in FLE of GO-PANI, monitored at 410 nm [Fig. 8(a)], clearly indicates the formation of a different emissive moiety in the ground state. But, the main absorption peak at about 276 nm of GO-PANI at pH = 1.8 is absent in the fluorescence excitation spectra. This implies that the main band gap absorption has no contribution to the fluorescence. Zhang et al observed similar type of observation indicating that the emission is not correlated to the band gap electronic transition in GO like nanomaterials [29]. Absence of significant intensity in the FLE spectrum of GO-PANI in alkaline pH, monitored at 410 nm, suggests that the species emitting at 410 nm has very little contribution at this region of pH [Fig. 8(b)]. Similarly, monitoring emission intensity at 345 nm in acidic pH, FLE spectrum does not exhibit any significant spectral pattern and this may be due to very little contribution of the species emitting at 345 nm at this pH [Fig. 8(a)].

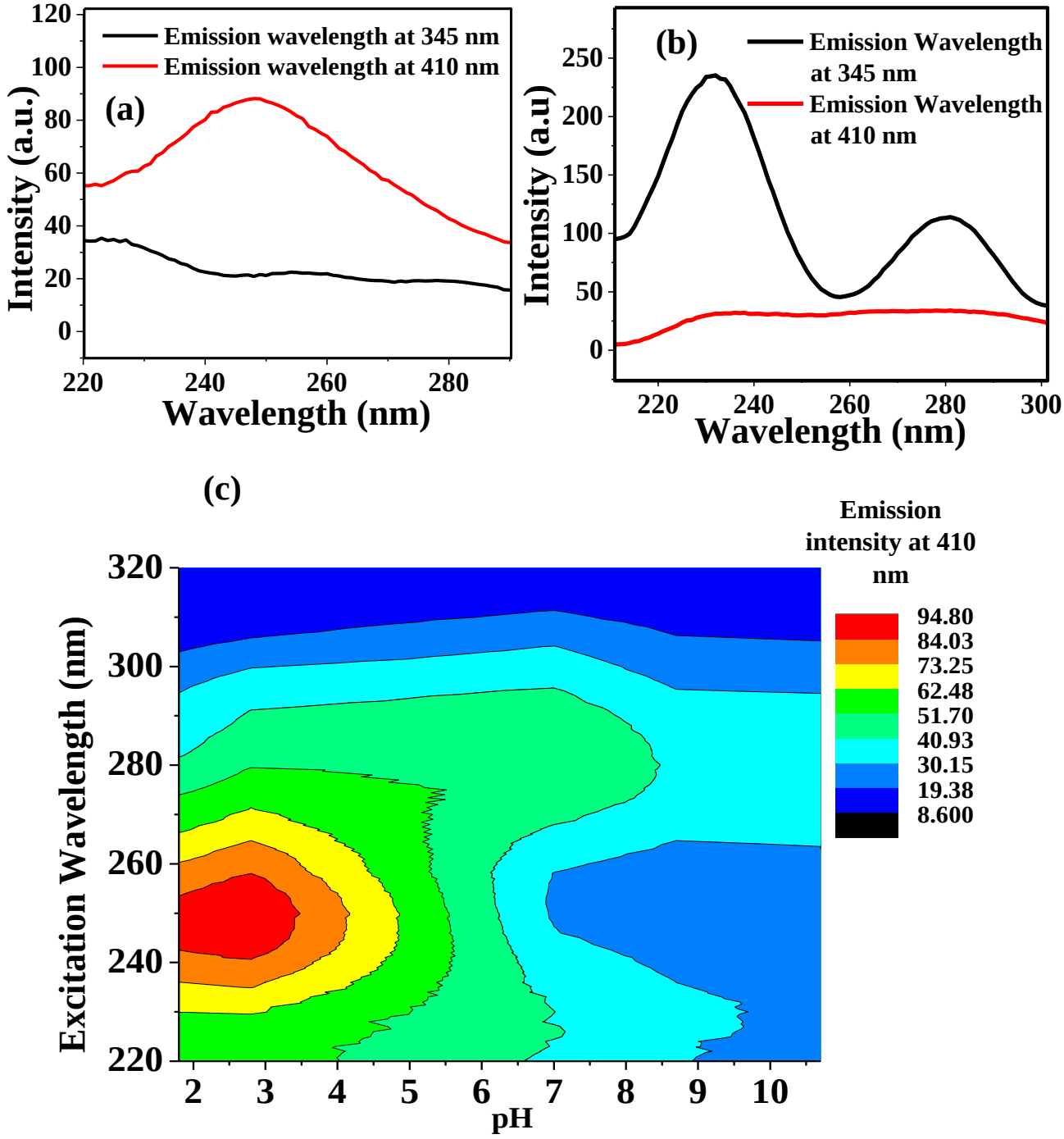

Fig. 8 Excitation spectra of the aqueous dispersion of GO-PANI (a) at pH = 1.8 (b) at pH = 10.7 (c) Excitation-emission matrices of GO-PANI at different pH (monitored at 410 nm)

The complete picture of the pH dependent emission band centered at 410 nm is represented by excitation emission matrices (EEM) of GO-PANI at different pH [Fig. 8(c)]. The EEMs of GO-PANI clearly shows that the emission centered at 410 nm is obtained by the excitation at 250 nm in low pH and this band gradually disappears with the increase in pH. The luminescence of GO arises from recombination of electron-hole pairs in localized electronic states originating from various possible configurations and the wavelength of fluorescence is determined by the size of sp^2 clusters [32]. According to Cushing et al, emissions from various species combine to create the broad fluorescence of GO [33]. The excitation wavelength and pH dependent emission of GO may be due to the superposition of fluorescence of different moieties with different relative intensities [17, 34]. Dual emission band (λ_{ex} = 280 nm) of the aqueous dispersion (pH = 4.6) of GO-PANI and the different nature of FLE at two different pH (1.8 and 10.7) clearly suggests the presence of two different fluorophoric species; one of them is formed only when the pH of the medium is acidic. The species emitting at ~ 345 nm is resembled to GO fluorophore, A, while the second one, B, emitting at ~ 410 nm, is only appeared in acidic pH (Fig. 4). The peak obtained in the FLE of GO-PANI monitored at 410 nm in acidic pH [Fig. 8(a)], is indicating that the second fluorophoric moiety, B, absorbs at ~ 250 nm. But, in the acidic pH, when the sample was excited at 280 nm, the obtained emission band at 410 nm may be due to the contribution of B as 280 nm is the red end of the absorption band of B. Here, it may be mentioned that the excitation of GO-PANI at 250 nm in acidic pH (less than 3) exhibits the same type of fluorescence spectrum as observed when the sample of GO-PANI is excited at 280 nm. The pH dependent steady state fluorescence properties of the aqueous dispersion of GO-PANI are summarized in Table 1.

Table 1

Excitation Wavelength	pH < 3 Dominating species: B Absorption peak ~ 250 nm	pH ~ 4 – 5 Both A and B may present with different contribution	pH ≥ 7 Dominating species: A Absorption peak ~ 230 nm
230 nm	Emission band centered at 410 nm	Emission band centered at 345 nm	Emission band centered at 345 nm
250 nm	Emission band centered at 410 nm	Emission band centered at 350 nm	Emission band centered at 350 nm
280 nm	Emission band centered at 410 nm	Dual emission at 345 nm and 405 nm	Emission band centered at 345 nm

4.3.5. Life Time of GO-PANI dispersion

Fig. 9(a) shows the fluorescence decays in logarithmic scale at 345 nm obtained by exciting the aqueous dispersion of GO-PANI at 280 nm. In the high pH region (7 and 10.7), the fluorescence decays are almost same and single exponential with life time 850 – 870 ps (Table 2). But, in acidic pH (1.8 and 4.6), the fluorescence decay at 345 nm are slightly different and bi-exponential [Fig. 9(a)] with maximum contribution (more than 95%) of the fast component of 940 - 950 ps (Table 2). The fluorescence decays in logarithmic scale of GO-PANI (λ_{ex} = 280 nm) at 410 nm was found to be dependent on pH of the medium [Fig. 9(b)]. In the high pH region (7 and 10.7), the major contributing (more than 90%) component is ~ 1 ns along with a slow component of ~ 6 ns (Table 2). But in the acidic medium, the fluorescence decays at 410 nm are multi-exponential with two components of ~ 2.5 – 3 ns and 5.3 – 5.7 ns in both pH (1.8 and 4.6) along with another component of 1 ns for the GO-PANI dispersion only at pH = 4.6 (Table 2). The disappearance of 1 ns component at pH = 1.8 in the fluorescence decay at 410 nm suggests the absence of the emissive moiety emitting at 345 nm in alkaline medium.

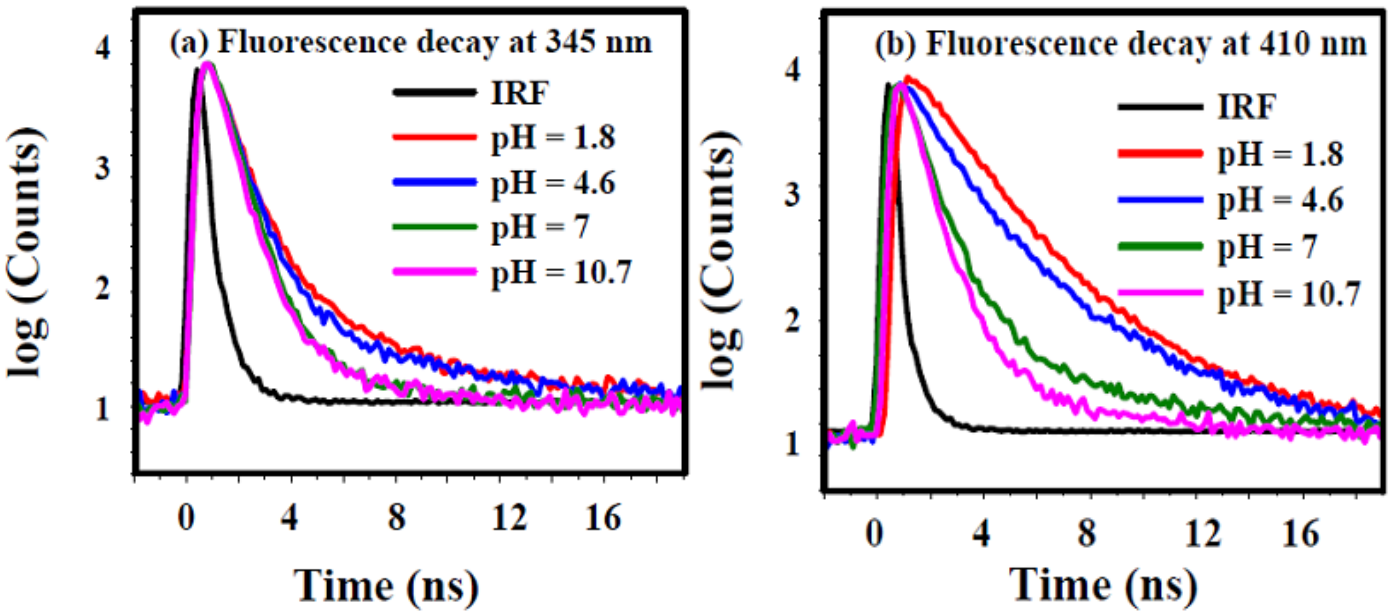

Fig. 9 Fluorescence decays of GO-PANI dispersions in logarithmic scale at different pH monitored at (a) 345 nm and (b) 410 nm

The presence of two different species in the aqueous dispersion (pH = 4.6) of GO-PANI nanocomposite is also manifested by the contribution of fluorescence life time components. The 1 ns components in the decays at 345 and 410 nm is possibly due to the species A and this component is completely disappeared at pH = 1.8. On the other hand, appearance of the 2.5 - 3 ns component and the long lived component (more than 5 ns) in the fluorescence decay at 410 nm may be due to a new species, B, formed in acidic pH and the contribution of these two components are about 1.5 times higher at pH = 1.8 compared to the pH = 4.6. This observation clearly suggests that with the decrease in pH of the medium formation of B by the charge transfer interaction between PANI and GO in the ground state becomes more favorable. The extent of this type of donor-acceptor interaction of PANI with the GO moiety may quantitatively be measured from the contribution of the fluorescence life time components (Table 2). In alkaline medium, the contribution of the long component (greater than 5 ns) of the fluorescence decay at 410 is negligibly small (less than 10%). But, in acidic medium, total

contribution of these two components (2.5 – 3 ns and 5.3 – 5.7 ns) of the decays at 410 nm are 80% and 100%, respectively. Thus, from the fluorescence life time data, we may conclude that the PANI fully interacted with GO at very low pH (<3).

Table -2

Fluorescence decay parameters of GO-PANI at different pH

λ_{ex}	pH of the medium	Fluorescence lifetime at 345 nm		Fluorescence lifetime at 410 nm		
280 nm	10.7	850 ps		τ_1 = 1.1 ns (97%)	τ_2 = 6.0 ns (3%)	
	7.0	870 ps		τ_1 = 1.2 ns (92%)	τ_2 = 5.9 ns (8%)	
	4.6	940 ps (96%)	6.0 ns (4%)	τ_1 = 1.0 ns (37%)	τ_2 = 3.0 ns (43%)	τ_3 = 5.7 ns (20%)
	1.8	945 ps (97%)	6.1 ns (3%)	τ_1 = 2.5 ns (65%)	τ_2 = 5.3 ns (35%)	

4.4. Conclusions

PANI grafted GO nanocomposite shows tunable fluorescence controlled by pH of the medium. For the first time aqueous dispersion of GO-PANI is exhibiting a remarkable change in fluorescence band from UV to visible region with the decrease in pH. Appearance of a new emission band in visible region at very low pH may be explained as a result of the formation of a ground state species by electron donor-acceptor interaction between emraldine salt form of PANI and GO along with π-π stacking interactions. Formation of this emissive species in the ground state is supported by the pH dependent emission spectra, fluorescence excitation spectra and life time data. This work may provide a further insight on the research of GO based pH sensing materials. Thus, the effect of pH on the luminescence properties of GO-PANI may

have implications in biological sensing and optoelectronics. The observed phenomenon of pH dependent fluorescence of GO-PANI may be extended to carbon quantum dots and other nanocomposites. Hence, this work indicates that the emission of GO-PANI is tuned by the pH of the medium and this is possibly the first report of such pH dependent tuning of fluorescence between UV and visible region. This interesting observation is attributed to the ground state charge transfer interaction by utilizing the polaron state of emeraldine salt form of PANI in the GO-PANI nanocomposite. The observed results shades light in the synthesis of tunable optoelectronic devices in aqueous phase and may open up various aspects of luminescence research of GO based novel functional materials.

4.5. Reference

[1] D. Cai, M. Song, *J. Mater. Chem.* 2010, **20**, 7906–7915.

[2] L. Nyholm, G. Nyström, A. Mihranyan, M. Strømme, *Adv. Mater.*, 2011, **23**, 3751–3769.

[3] A. G. MacDiarmid, *Angew. Chem. Int. Ed*, 2001, **40**, 2581-2590.

[4] D. Li, J. Huang, R. B. Kaner, *Acc. Chem. Res*., 2009, **42**, 135-145.

[5] J. Stejskal, R.G. Gilbert, *Pure Appl. Chem*, 2002, **74**, 857-867.

[6] K. Lee, S. Cho, S. H. Park, A. J. Heeger, C. W. Lee, S. H. Lee, *Nature*, 2006, **441**, 65-68.

[7] J. Yan, T. Wei, B. Shao, Z. Fan, W. Qian, M. Zhang, F. Wei, *Carbon*, 2010, **48**, 487–493.

[8] R. Wang, S. Wang, D. Zhang, Z. Li, Y. Fang, X. Qiu, *ACS Nano*, 2011, **5**, 408-412.

[9] U. Rana, S. Malik, *Chem. Comm.*, 2012, **48**, 10862–10864.

[10] K. Zhang, L. Zhang, X. S. Zhao, J. Wu, *Chem. Mater*, 2010, **22**, 1392–1401.

[11] S. M. Imran, Y. N. Kim, G. N. Shao, M. Hussain,Y. Choa, H. T. Kim, *J. Mater. Sci.*, 2014, **49**, 1328–1335.

[12] N. Yang, J. Zhai, M. Wan, L. Jiang *Synth. Met.*, 2010, **160**, 1617–1622.

[13] Y. Zhao, G-S. Tang, Z–Z. Yu, J-S. Qi, *Carbon*, 2012, **50**, 3064–3073.

[14] C. Vallés, P. Jiménez, E. Muñoz, A. M. Benito, W. K. Maser, *J. Phys. Chem. C*, 2011, **115**, 10468-10474.

[15] N. A. Kumar, H.-J. Choi, Y. R. Shin, D. W. Chang, L. Dai, J.-B. Baek, *ACS Nano*, 2012, **6**, 1715-1723.

[16] P. R. Bevington, Data Reduction and Error Analysis for the Physical sciences, McGraw Hill, New York, 1969.

[17] P. Dutta, D. Nandi, S. Datta, S. Chakraborty, N. Das, S. Chatterjee, U. C. Ghosh, A. Halder, *J. Lumin.*, 2015, **168**, 269-275.

[18] S. Liu, X. Liu, Z. Li, S. Yang, J. Wang, *New J. Chem.*, 2011, **35**, 369-374.

[19] J. Wang, H. Xian, T. Peng, H. Sun, F. Zheng, *RSC Adv.*, 2015, **5**, 13607-13612.

[20] A. K. G. Tapia, K. Tominaga, *Chem. Phys. Lett*., 2014, **598** 39-42.

[21] Y.-Q. Li, T. Yu, T.-Y. Yang, L.-X. Zheng, K. Liao, *Adv. Mater*, 2012, **24**, 3426-3431.

[22] D. D. Nicolas, E. F. Poncin, Anal. *Chim. Acta*., 2003, **475**, 1-15.

[23] G. G. Wallace, G. M. Spinks, L.A.P. Kane-Maguire, P. R. Teasdale, Conductive Electroactive Polymers: Intelligent Polymer Systems, CRC Press, London, 2009.

[24] K. M. Molapo, P. M. Ndangili, R. F. Ajayi, G. Mbambisa, S. M. Mailu, N. Njomo, M. Masikini, P. Baker, E. I. Iwuoha, *Int. J. Electrochem. Sci*., 2012, **7**, 11859-11875.

[25] J. E. de Albuquerque, L. H. C. Mattoso, R. M. Faria, J. G. Masters, A.G, MacDiarmid, *Synth. Met.*, 2004, **146**, 1-10.

[26] H. S. Fan, H. Wang, N. Zhao, J. Xu, F. Pan, *Sci. Rep*., 2014, **4**, 7426.

[27] G. G. Wallace, G. M. Spinks, P. R. Teasdale, Conductive Electroactive Polymers, CRC Press, London, 2002.

[28] S. Stafström, J. L. Brédas, A. J. Epstein, H. S. Woo, D. B. Tanner, W. S. Huang, A. G. MacDiarmid, *Phys. Rev. Lett.*, 1987, **59**, 1464-1467.

[29] X-F. Zhang, X. Shao, S. Liu, *J. Phys. Chem. A*, 2012, **116**, 7308-7313.

[30] M. Pumera, *Chem. Rec.*, 2009, **9**, 211-223.

[31] M. S. Dresselhaus, G. Dresselhaus, *Adv. Phys*., 2002, **51**, 1-186.

[32] K. P. Loh, Q. Bao, G. Eda, M. Chhowalla, *Nat. Chem*., 2010, **2**, 1015-1024.

[33] S. K. Cushing, M. Li, F. Huang, N. Wu, ACS Nano, 2014, **8**, 1002–1013.

[34] J. Shang, L. Ma, J. Li, W. Ai, T. Yu, G. G. Gurzadyan, *Sci. Rep*., 2012, **2(792)**, 1–8.